Dalton Transactions

Accepted Manuscript

This is an *Accepted Manuscript*, which has been through the Royal Society of Chemistry peer review process and has been accepted for publication.

Accepted Manuscripts are published online shortly after acceptance, before technical editing, formatting and proof reading. Using this free service, authors can make their results available to the community, in citable form, before we publish the edited article. We will replace this *Accepted Manuscript* with the edited and formatted *Advance Article* as soon as it is available.

You can find more information about *Accepted Manuscripts* in the Information for Authors.

Please note that technical editing may introduce minor changes to the text and/or graphics, which may alter content. The journal's standard Terms & Conditions and the Ethical guidelines still apply. In no event shall the Royal Society of Chemistry be held responsible for any errors or omissions in this *Accepted Manuscript* or any consequences arising from the use of any information it contains.

ROYAL SOCIETY OF CHEMISTRY

www.rsc.org/dalton

Journal Name

RSCPublishing

COMMUNICATION

Preparation of solid-solution type Fe–Co nanoalloys by synchronous deposition of Fe and Co using dual arc plasma guns

Cite this: DOI: 10.1039/x0xx00000x

Received ooth January 2012,
Accepted ooth January 2012

DOI: 10.1039/x0xx00000x

www.rsc.org/

Masaaki Sadakiyo,[a,b] Minako Heima,[a,b] Tomokazu Yamamoto,[c] Syo Matsumura,[c] Masashi Matsuura,[d] Sugimoto Satoshi,[d] Kenichi Kato,[b,e] Masaki Takata,[e] and Miho Yamauchi*[a,b,f]

We succeeded in the efficient preparation of well-dispersed Fe–Co nanoalloys (NAs) using the arc plasma deposition method. Synchronous shots of dual arc plasma guns were applied to a carbon support to prepare the solid-solution type Fe–Co NAs having an approximately 1:1 atomic ratio. The alloy structures with and without a reductive thermal treatment under hydrogen atmosphere were examined using X-ray powder diffraction, scanning transmission electron microscopy (STEM) combined with energy-dispersive X-ray analysis, high resolution STEM, and magnetic measurements, suggesting that highly crystalline spherical particles of ordered B2-type Fe–Co NAs form by the thermal treatment of the deposited grains.

Development of an efficient preparation of designed nanoalloys (NAs) is an important challenge in materials science because of their useful applications, such as catalysts,[1] magnets,[2] and optical materials.[3] So far, metallic NAs immobilized on a support have been prepared using various methods, such as co-impregnation,[4] microemulsion,[5] simultaneous reduction,[6] and so on. Recently, an arc plasma deposition (APD) method[7] has been used for large-scale (>1 g) and solvent-free synthesis of well-dispersed metal nanoparticles on a support. Some metals or metal oxides deposited on supports have been prepared using the APD method (e.g., Pt/TiO_2).[8] However, there are few reports on the preparation of metallic NAs using the APD method.[9] In this study, we focus especially on an application of the APD method for the preparation of Fe–Co NAs, which have potential interest not only as catalysts[10] but also as magnetic materials.[11] Iron group NAs, including Fe–Co easily aggregate, which prevents the preparation of well-dispersed nanoparticles less than a few tens of nanometres in diameter.[10] We employed synchronous deposition of Fe and Co with an APD instrument equipped with dual arc plasma guns, as illustrated in Figure 1. In this experimental set-up, metal compositions and alloy structures are potentially variable by changing the number of shots or the shot sequence. In simultaneous shooting, Fe and Co plasma species are synchronously showered on a support from both metal targets. However, it is not possible to tell the structure, morphology, and size of the surface species. Here, we report the first successful preparation of well-dispersed Fe–Co NAs using the ADP method without any protecting agent and present detailed structures and elemental distributions of Fe–Co products formed on active carbon for the production of favourable NA using the APD method.

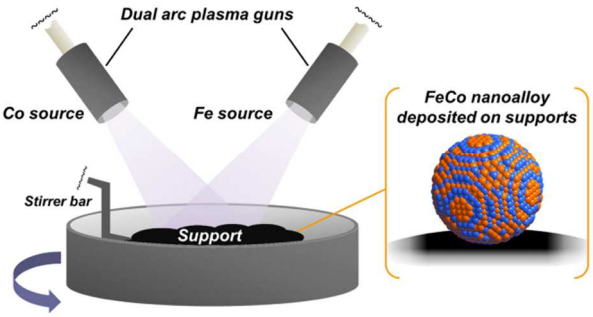

Fig. 1 Schematic view of the preparation method for Fe–Co NAs deposited on a support using synchronous shots of dual arc plasma guns equipping Fe and Co sources.

Fe–Co NAs were prepared using synchronous shots of dual arc plasma guns (ULVAC ADP-3P-N2) equipping Fe and Co metals onto carbon supports. The carbon support (Vulcan XC-72R, 1.07 g) was placed in a pot inside the vacuum chamber of the equipment and was continuously stirred by rotation of the pot at 30 rpm with a stirrer bar during the deposition process. Quantities of 1000 (abbreviated to **FeCo^{1000}**), 5000 (**FeCo^{5000}**), and 30000 (**FeCo^{30000}**) synchronous plasma shots (500, 2500, and 15000 shots for each metal) were discharged from the arc plasma guns at a frequency of 10 Hz under vacuum conditions to obtain various samples having different metal amounts. The pot was maintained at 18 °C using a water-cooling apparatus. After the discharges, black powders were obtained for each sample.

Metal loadings and atomic ratios of the deposited Fe and Co atoms were examined using inductively coupled plasma–atomic emission spectrometry (ICP–AES, Thermo iCAP6300). The amounts of metals in **FeCo^{1000}**, **FeCo^{5000}**, and **FeCo^{30000}** were estimated to be 0.086, 0.350, and 1.81 wt%, respectively. As shown in Figure S1, the deposited weights of each Fe or Co metal were proportional to the number of shots from each arc plasma gun.

Dalton Transactions Accepted Manuscript

Irradiation rates of Fe and Co sources were represented with similar proportional constants, resulting in almost 50:50 atomic ratios of Fe and Co in the prepared specimens; i.e., the atomic ratios of Fe and Co in **FeCo^{1000}**, **FeCo^{5000}**, and **FeCo^{30000}** were determined to be 53:47, 48:52, and 54:46, respectively, as shown in Figure S2. These results are probably attributable to analogous kinetic phenomena involved in plasma formations of the two metals due to their similar fundamental parameters of the two metals—e.g., molar masses (M(Fe) = 55.8, M(Co) = 58.9 g mol^{-1}) and boiling points of Fe and Co (3134 and 3200 K, respectively)—and ensure favourable controllability for Fe and Co compositions on the support in applying the ADP method.

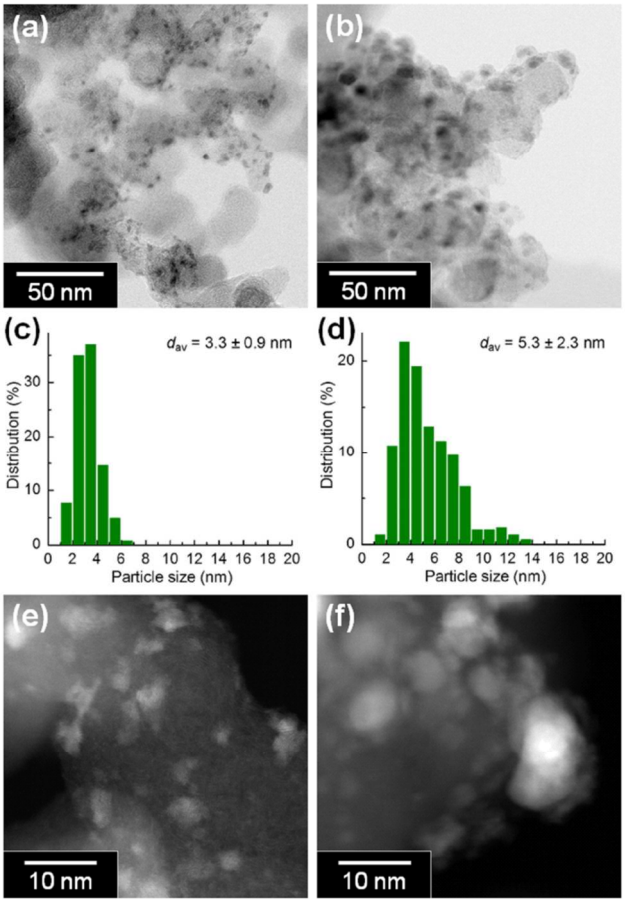

Fig. 2 STEM images of (a) **FeCo^{5000}** and (b) **FeCo^{30000}**. Particle size distributions of (c) **FeCo^{5000}** and (d) **FeCo^{30000}**. HAADF–STEM images of (e) **FeCo^{5000}** and (f) **FeCo^{30000}**.

To identify distributions of the deposited Fe and Co atoms on the support, we performed scanning transmission electron microscope (STEM, JEOL JEM-ARM 200F) observations. On **FeCo^{1000}**, clear images of metal species were not obtained because of sparseness of the metal atoms, suggesting that metal loadings less than 0.1 wt% are insufficient to attain a metal density for grain formation among Fe and Co species. In contrast, we could see particle formation on **FeCo^{5000}** and **FeCo^{30000}** samples as deposited (Figure 2) although some parts of supports remain bare surfaces (Figure S3–S4). Two reasons for this inhomogeneous distribution of metal species are considerable. The first reason is that an excess amount of support volume for the amount of sprayed plasma species is required in the mechanically stirring system for its stable operation. As the second one, we think that agglomerations of the carbon supports are not sufficiently disaggregated by the mechanical stirring and plasma species are sprayed only on the surface of the agglomerations, i.e., the inside of the agglomerations remain non-contact with the plasma, resulting in relatively high content of the metal species showed in the STEM images compared with those determined by ICP measurements which reflect loading amounts of metal species in the whole sample including unmodified support portions. Nevertheless, observed images rightly reflect a growth process of the irradiated metal species. The mean diameters of the particles on **FeCo^{5000}** and **FeCo^{30000}** were estimated to be 3.3 and 5.3 nm, respectively, (Figures 2c–d) by counting over 200 particles on the STEM images. This result indicates that the size of the particles composed of metal elements increases with the number of shots.

Crystallinities of the particles were examined using a high resolution STEM (HR-STEM) technique. We could only see amorphous grains in **FeCo^{5000}** but not find crystalline ones as shown in Figure S5a. In contrast, some crystalline parts with lattice fringes existed in **FeCo^{30000}** (Figure S5b), while most of parts were amorphous. The distance between the fringes in the Figure S5b was estimated to be 0.20 nm, corresponding to 0.202 nm of the interlayer distance of (110) planes of the bcc or B2 structure which is the most stable phase of Fe–Co alloy having an atomic ratio around 1:1 at ambient temperature.[12] This observation represents that metallic particles are prepared by the APD method. We think that the amorphous part is attributable to mixed oxide for the reason discussed later. To confirm the crystal structure of the whole particles, we conducted X-ray powder diffraction (XRPD) measurements (RIKEN Materials Science Beamline BL44B2 at SPring-8,[13] λ = 0.5004 Å). Figure S6 shows XRPD patterns of **FeCo^{1000}**, **FeCo^{5000}**, and **FeCo^{30000}**. As seen in the HR-STEM images, **FeCo^{5000}** (and **FeCo^{1000}**) did not show any obvious diffraction patterns from metallic phases, such as Fe, Co, nor Fe–Co alloy, due to the amorphous nature of the samples. In the case of **FeCo^{30000}**, there was only a small peak around 14.2°, which is attributable to the diffraction from the (110) plane of bcc or B2 phase. These results imply that Fe-group metallic particles with diameters less than approximately 5 nm do not remain in the air due to their high surface reactivity with oxygen, even if metallic particles are formed in the vacuum chamber.

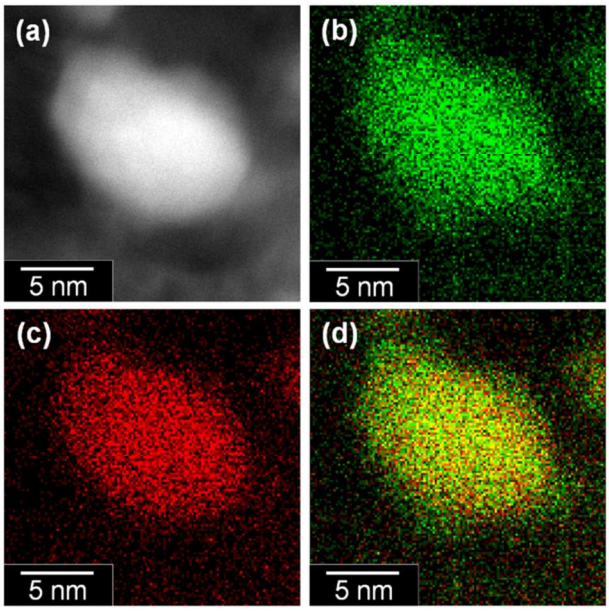

Dalton Transactions Accepted Manuscript

This journal is © The Royal Society of Chemistry 2012

Fig. 3 (a) HAADF–STEM image of a grain of **FeCo**^{30000}. STEM–EDX map of (b) Fe-K and (c) Co-K signals. (d) Overlap image of Fe-K and Co-K signals. Green and red correspond to Fe-K and Co-K signals, respectively.

We examined elemental distributions on **FeCo**^{5000} and **FeCo**^{30000} using STEM combined with energy-dispersive X-ray analyses (STEM–EDX, JEOL JEM-ARM 200F). Figures 3 and S7 show STEM–EDX maps for grains of **FeCo**^{30000} and **FeCo**^{5000} as deposited, respectively. EDX signals of both Fe-K and Co-K lines were homogeneously distributed in a grain, indicating that the atoms deposited by the synchronous shots of the dual arc plasma guns automatically formed alloy grains on the carbon support. Figures 3d and S7d describe the overlap intensity of these Fe-K and Co-K signals. On both specimens, Fe and Co atoms form neither a phase separation nor a core–shell-type alloy but a solid-solution-type alloy on the active carbon; even the shape of the grains is not spherical. As shown in Figure S8, other grains in **FeCo**^{30000} also include both Fe and Co atoms.

Then, we treated all specimens at 800 °C for 1 minute under 5% H_2/Ar mixed gas flow, namely, hydrogen treatment for the formation of crystalline particles. XRPD patterns of **FeCo**^{1000} before and after hydrogen treatment, as shown in Figure S9, seem to be almost identical to that of the carbon support. However, in the cases of **FeCo**^{5000} and **FeCo**^{30000}, we could recognize the existence of crystalline Fe–Co alloys after the hydrogen treatment (Figures S10–S11). Figure S11 provides the XRPD patterns of the **FeCo**^{30000} before and after hydrogen treatment. As mentioned above, the bulk Fe–Co alloy with the atomic ratio of 1:1 is known to show bcc or B2 structure below 700 °C.[12] The hydrogen-treated **FeCo**^{30000} showed clear diffraction peaks around 14.2° (110), 20.2° (200), and 24.8° (211) derived from the bcc or B2 structure, implying that hydrogen treatment induced rearrangement of Fe and Co atoms to form crystalline metal nanoparticles. We cannot assign the crystal structure to whether a bcc or B2 type because the characteristic peak of the 100 plane was not recognized because of the weakness of the peak. However, the hydrogen-treated samples formed an ordered B2 structure, which was confirmed by HR-STEM observations as discussed below. As shown in Figure S10, the hydrogen-treated **FeCo**^{5000} also showed a very weak peak around 14.2°, while no peak was observed before the hydrogen treatment, implying that the rearrangement of Fe and Co atoms or particle growth also occurred as in the case with **FeCo**^{30000}.

Figure S12 shows STEM and HAADF–STEM images of the hydrogen-treated samples of **FeCo**^{5000} and **FeCo**^{30000}. In both cases, odd-shaped particles observable on the pristine samples were clearly changed to spherical form with relatively smooth surfaces, indicating that rearrangement of Fe and Co atoms on the carbon support occurs during the hydrogen treatment. The mean diameters of the whole particle including both oxide and metallic parts were also changed by hydrogen treatment and were determined to be 8.3 and 8.8 nm for **FeCo**^{5000} and **FeCo**^{30000}, respectively, as shown in Figure S12c–d. This result indicates that particle growth also occurred during the hydrogen treatment. However, the similarity in the particle sizes of both samples gives us a good opportunity to prepare catalysts having various or optimal amounts of metals on supports without drastic changes in the diameter of the metal species. Note that the particles after hydrogen treatment had core–shell-like structures (Figures S12e–f), where the shell is amorphous. More-detailed observations were conducted using a HR-STEM technique as shown in Figures 4a–b. Both the hydrogen-treated **FeCo**^{5000} and **FeCo**^{30000} provide similar lattice images consisting of a crystalline core and an amorphous shell. We could see clear lattice planes such as (110) and (200) planes of the B2-type crystal structure, indicating that the highly crystalline metallic particles were formed by the hydrogen treatment. This result suggests that the surface of the nanoparticles was oxidized during experimental manipulations due to a high reactivity of the FeCo alloy with oxygen. We also think that the amorphous part of as-deposited **FeCo**^{5000} and **FeCo**^{30000} was obtained through oxidation of the deposited FeCo alloys. In fast Fourier transform (FFT) images of the HR-STEM images (Figures S13-S14), we could recognize the characteristics peaks of an ordered B2 structure, e.g. (100) plane, confirming that the ordered B2-type NAs were efficiently prepared through the APD operation and the additional hydrogen treatment.

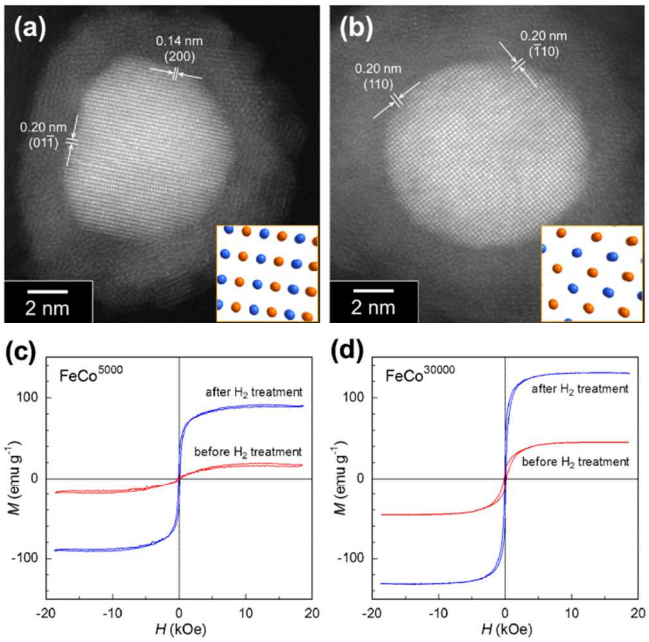

Fig. 4 HR–STEM images of the hydrogen-treated (a) **FeCo**^{5000} and (b) **FeCo**^{30000}. The insets in (a) and (b) show the B2 crystal structure of FeCo alloy viewed along [011] and [001] directions (corresponding to the direction along the incident electron beam), respectively. Room-temperature magnetizations of (c) **FeCo**^{5000} and (d) **FeCo**^{30000} before (red) and after (blue) the hydrogen treatment.

To confirm the elemental composition of these particles, we also performed STEM–EDX analyses for the hydrogen-treated samples of **FeCo**^{5000} and **FeCo**^{30000}. Figures S15 and S16 show STEM–EDX maps for particles of hydrogen-treated **FeCo**^{5000} and **FeCo**^{30000}, respectively. In both cases, EDX signals from both Fe-K and Co-K lines were homogeneously distributed in a particle. This result is consistent with the fact that Fe and Co atoms are alternatively arranged, i.e., B2-type structure forms in the particles. Figures S17 and S18 show line profiles of EDX signals for **FeCo**^{5000} and **FeCo**^{30000}, respectively. Both signals from Fe and Co atoms showed a similar distribution because of their B2-type arrangement. However, distributions of O-K signals in these samples were different from those of the Fe-K and Co-K signals. The profile of the O-K signals clearly showed that peaks were located around the surface region of the particle, confirming that the centre of the particle consisted of Fe–Co metallic NAs and that the outside was amorphous oxide, which accords with the above discussion

Dalton Transactions Accepted Manuscript

regarding STEM images of **FeCo^{5000}** and **FeCo^{30000}** after hydrogen treatment. To estimate the metallic part of FoCo alloys, we also performed magnetic measurements as shown in Figures 4c–d. Saturated magnetizations of FeCo alloys in **FeCo^{5000}** and **FeCo^{30000}** as prepared and **FeCo^{5000}** and **FeCo^{30000}** with hydrogen treatments were estimated to be 17, 45, 91, and 131 emu g^{-1}, respectively. These magnetization values are considerably smaller than 233 emu g^{-1} of the $Fe_{50}Co_{50}$ metallic nanocrystal,[14,15] suggesting that samples do not purely consist of the metallic FeCo alloys. If we hypothesize that the grains in **FeCo^{5000}** before the hydrogen treatment, which exhibits 17 emu g^{-1} of saturated magnetization, are purely composed of mixed oxide, the amounts of metallic part in **FeCo^{5000}** and **FeCo^{30000}** after the H_2 treatments are estimated to be approximately 35 and 54 wt% from the calculation based on the weight of the included Fe and Co atoms, confirming that the existence of both metallic and oxide parts in these samples. From these results, we could conclude that well-dispersed ordered B2-type Fe–Co alloy nanoparticles having a mean diameter of less than 10 nm were successfully prepared through synchronous shots from the dual arc plasma guns and the hydrogen treatment without any chemical reagents and solvents, and the surface of the Fe–Co alloys tends to be coated with a thin oxide layer. Note that this is the first example of ordered NAs synthesis through APD method and detailed observation for NAs formation through the ADP method although an example of preparation of a Pd–Fe catalyst has been reported.[9]

In summary, we have demonstrated that the APD method is a new method for efficient preparation of well-dispersed Fe–Co NAs on a support without protecting agent, solvents, or any reagents. We have prepared an Fe–Co NA supported on carbon using the APD method with synchronous shots of the arc plasma guns. Small NAs having mean diameters of less than 10 nm were successfully dispersed on the support without any protecting agent. We found that the Fe and Co atoms deposited using arc plasma guns aggregate with each other to form non-spherical Fe–Co alloy grains with low crystallinity on the carbon support and that hydrogen treatment at 800 °C caused rearrangements of the atoms and particle growth to form spherical Fe–Co metal NAs with ordered B2 structure. These results are a useful example of the efficient preparation of iron-group NAs and will provide a new methodology to prepare bimetallic catalysts with various supports.

Acknowledgements

This work was supported by JST-CREST and JSPS KAKENHI Grant Numbers 25288030 and 24655040.

Notes and references

[a] *International Institute for Carbon-Neutral Energy Research (WPI-I2CNER), Kyushu University, 744 Moto-oka, Nishi-ku, Fukuoka 819-0395, Japan. E-mail: yamauchi@i2cner.kyushu-u.ac.jp; Fax: +81 92-802-6874; Tel: +81 92-802-6874*

[b] *Core Research for Evolutional Science and Technology (CREST), Japan Science and Technology Agency (JST), 7 Goban-cho, Chiyoda-ku, Tokyo 102-0076, Japan*

[c] *Department of Applied Quantum Physics and Nuclear Engineering, Kyushu University, 744 Moto-oka, Nishi-ku, Fukuoka 819-0395, Japan*

[d] *Department of Materials Science, Graduate School of Engineering, Tohoku University, 6-6-02 Aramaki Aza Aoba, Aoba-ku, Sendai 980-8579, Japan*

[e] *RIKEN SPring-8 Center, 1-1-1 Kouto, Sayo-cho, Sayo-gun, Hyogo 679-5148, Japan.*

[f] *Department of Chemistry, Faculty of Science, Kyushu University, Hakozaki 6-10-1, Higashi-ku, Fukuoka 812-8581, Japan*

† Electronic Supplementary Information (ESI) available: Experimental details and supporting results. See DOI: 10.1039/c000000x/

1 D. A. Slanac, W. G. Hardin, K. P. Johnston, K. J. Stevenson, *J. Am. Chem. Soc.* **2012**, *134*, 9812–9819.; S. Xie, H. Tsunoyama, W. Kurashige, Y. Negishi, T. Tsukuda, *ACS catal.* **2012**, *2*, 1519–1523.

2 J.-I. Park, M. G. Kim, Y.-W. Jun, J. S. Lee, W.-R. Lee, J. Cheon, *J. Am. Chem. Soc.* **2004**, *126*, 9072–9078. I. Robinson, S. Zacchini, L. D. Tung, S. Maenosono, N. T. K. Thanh, *Chem. Mater.* **2009**, *21*, 3021–3026.

3 M. B. Cortie, A. M. McDonagh, *Chem. Rev.* **2011**, *111*, 3713–3735.

4 L. Piccolo, S. Nassreddine, M. Aouine, C. Ulhaq, C. Geantet, *J. Catal.* **2012**, *292*, 173–180.

5 A. Habrioux, W. Vogel, M. Guinel, L. Guetaz, K. Servat, B. Kokoh, N. Alonso-Vante, *Phys. Chem. Chem. Phys.* **2009**, *11*, 3573–3579.

6 S. Link, Z. L. Wang, M. A. El-Sayed, *J. Phys. Chem. B* **1999**, *103*, 3529–3533.

7 H. Randhawa, *Thin Solid Films* **1988**, *167*, 175–185.; P. C. Johnson, H. Randhawa, *Surface and Coatings Technology* **1987**, *33*, 53–62.

8 T. Fujitani, I. Nakamura, T. Akio, M. Okumura, M. Haruta, Angew. Chem. 2009, 121, 9679–9682.; T. Ito, M. Kunimatsu, S. Kaneko, Y. Hirabayashi, M. Soga, Y. Agawa, K. Suzuki, *Talanta* **2012**, *99*, 865–870.; S. H. Kim, C.-H. Jung, N. Sahu, D. Park, J. Y. Yun, H. Ha, J. Y. Park, Appl. *Catal. A* **2013**, *454*, 53–58.; S. Hinokuma, M. Okamoto, E. Ando, K. Ikeue, M. Machida, *Catal. Today* **2011**, *175*, 593–597.; K. Qadir, S. H. Kim, S. M. Kim, H. Ha, J. Y. Park, *J. Phys. Chem. C* **2012**, *116*, 24054–24059.

9 S. Hinokuma, Y. Katsuhara, E. Ando, K. Ikeue, M. Machida, *Catal. Today* **2013**, *201*, 92–97.

10 T. Matsumoto, M. Sadakiyo, M. L. Ooi, S. Kitano, T. Yamamoto, S. Matsumura, K. Kato, T. Takeguchi, M. Yamauchi, *Scientific Reports* **2014**, *4*, 5620.; J. A. Amelse, L. H. Schwartz, J. B. Butt, *J. Catal.* **1981**, *72*, 95–110.; K. B. Arcuri, L. H. Schwartz, R. D. Piotrowski, J. B. Butt, *J. Catal.* **1984**, *85*, 349–361.

11 I. Robinson, S. Zacchini, L. D. Tung, S. Maenosono, N. T. K. Thanh, *Chem. Mater.* **2009**, *21*, 3021–3026.; A. Hütten, D. Sudfeld, I. Ennen, G. Reiss, K. Wojczykowski, P. Jutzi, *J. Mag. Mag. Mater.* **2005**, *293*, 93–101.; G. Reiss, A. Hütten, *Nature Mater.* **2005**, *4*, 725–726.

12 I. Ohnuma, H. Enoki, O. Ikeda, R. Kainuma, H. Ohtani, B. Sundman, K. Ishida, *Acta Materialia* **2002**, *50*, 379–393.; H. Asano, Y. Bando, N. Nakanishi, S. Kachi, *Trans. JIM* **1967**, *8*, 180–185.

13 K. Kato, R. Hirose, M. Takemoto, S. Ha, J. Kim, M. Higuchi, R. Matsuda, S. Kitagawa, M. Takata, *AIP Conference Proceedings* **2010**, *1234*, 875–878.

14 N. Poudyal, C. Rong, Y. Zhang, D. Wang, M. J. Kramer, R. J. Hebert, J. P. Liu, *J. Alloy Compound* **2012**, *521*, 55–59.

15 M. J. Sharif, M. Yamauchi, S. Toh, S. Matsumura, S. Noro, K. Kato, M. Takata, T. Tsukuda, *Nanoscale* **2013**, *5*, 1489–1493.

Dalton Transactions Accepted Manuscript

 This journal is © The Royal Society of Chemistry 2012